J. Plasma Physics (1999), *vol.* 61, *part* 3, *pp.* 407–414. Printed in the United Kingdom
© 1999 Cambridge University Press

Open boundary particle simulation of electrostatic ion cyclotron instability

SEIJI ISHIGURO,[1⋆] TETSUYA SATO,[2]
HISANORI TAKAMARU[2] and the
Complexity Simulation Group[2⋆⋆]

[1] Department of Electronic Engineering, Tohoku University, Aobayama 05, Sendai 980-8579, Japan

[2] Theory and Computer Simulation Center, National Institute for Fusion Science, 322-6 Oroshi-cho, Toki, Gifu 509-5292, Japan

(Received 1 June 1998)

We have developed a $2\frac{1}{2}$-dimensional open boundary particle simulation model and have studied the current-driven electrostatic ion-cyclotron instability and related d.c. potential difference. Fresh streaming electrons are injected smoothly from the boundaries at each time step, avoiding unphysical accumulation of charged particles in front of the boundaries. As a current-driven electrostatic ion cyclotron instability grows, a d.c. potential difference along the magnetic field lines is created.

1. Introduction

There is growing interest in particle simulation modelling including particle absorption and emission at boundaries. In the 1980s, Birdsall and co-workers developed bounded plasma modelling, and studied sheath and related plasma–wall interactions in front of solid walls or electrodes (Birdsall and Langdon 1985). They also studied plasma phenomena observed in Q machines.

On the other hand, the above method, in which particles are injected into the system without correlation of outgoing particles, is not appropriate for cases in which a local system is connected smoothly to an external plasma system. Although there were some attempts to treat such boundary conditions, it was reported that an undesirable effect appears near the boundary (Barnes et al. 1985).

Recently, Takamaru et al. (1997; see also Sato et al. 1995) have succeeded in developing an open boundary model in which the internal plasma is continuously and smoothly connected to an external plasma source such as a current generator. This model is applicable to the auroral field-line region in which fresh streaming electrons along the magnetic field lines are supplied from the plasma sheet.

Oscillations around the ion cyclotron frequency have been observed in magnetized plasmas in both space and the laboratory. D'Angelo and Motley (1962; see also Motley and D'Angelo 1963) reported the first clear-cut observation of these oscillations in a laboratory plasma. The oscillations were induced by applying a positive

⋆ Present address: Theory and Computer Simulation Center, National Institute for Fusion Science, 322-6, Oroshi-cho, Toki, Gifu 509-5292, Japan.

⋆⋆ K. Watanabe, R. Horiuchi, T. Hayashi, Y. Todo, T.-H. Watanabe and A. Kageyama.

https://doi.org/10.1017/S0022377899007539 Published online by Cambridge University Press

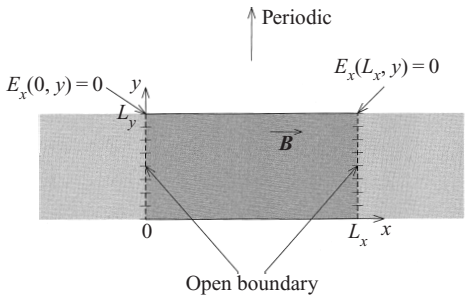


Figure 1. Schematic view of simulation configuration.

potential to a small disc electrode immersed in a single-ended Q machine. An electric current was generated along magnetic field lines, and thus the oscillations were considered to be caused by the current-driven electrostatic ion cyclotron instability predicted by Drummond and Rosenbluth (1962). Many detailed measurements were subsequently performed (Rynn et al. 1974; Correll et al. 1975; McWilliams et al. 1986).

In space plasmas, oscillations around the ion cyclotron frequency have also been observed (Kintner et al. 1978, 1979). Ion cone formation and d.c. potential difference associated with ion heating have been discussed in connection with the current-driven electrostatic ion cyclotron instability. In particular, it has been reported that a V-shaped potential structure and electrostatic ion cyclotron waves are simultaneously present above the auroral ionosphere (Mozer et al. 1977).

Although many numerical simulations have revealed growth of current-driven electrostatic ion cyclotron instability, saturation, and ion perpendicular heating (Okuda et al. 1981; Pritchett et al. 1981), they have not demonstrated the creation of a d.c. potential difference along the magnetic field lines by the instability.

In this paper, we present an extension of the open boundary particle simulation model for a two-dimensional configuration, and show that a current-driven electrostatic ion cyclotron instability grows and creates a d.c. potential difference.

2. Open boundary particle simulation model

We have developed a $2\frac{1}{2}$-dimensional open-boundary particle simulation model by adopting the method developed by Takamaru et al. (1997) for a one-dimensional simulation. For the time integration and the particle weighting, we use the standard particle-in-cell (PIC) simulation method (Birdsall and Langdon 1985), in which the leap frog time integration method and first-order particle weighting are used.

Figure 1 shows a schematic view of the simulation configuration of the $2\frac{1}{2}$-dimensional open-boundary particle model. The left and right boundaries are open, whereas a periodic boundary condition is applied in the y direction. The system is assumed to be divided into segments in the y direction, where each segment is assumed to be connected to an external constant current generator. We can specify a different velocity distribution function in each segment, and we assume that the velocity distribution function of the ith segment is $f^i(v_x, v_y, v_z)$. The net flux crossing the boundaries of the ith segment is given by

$$\Gamma^i = \int_{-\infty}^{\infty}\int_{-\infty}^{\infty}\int_{-\infty}^{\infty} v_x f^i(v_x, v_y, v_z)\, dv_x\, dv_y\, dv_z.$$

https://doi.org/10.1017/S0022377899007539 Published online by Cambridge University Press

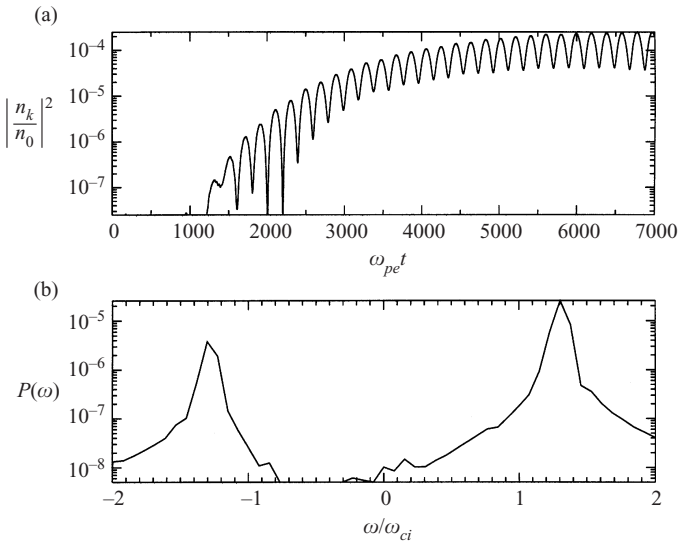


Figure 2. Time history of the ion density fluctuation (a) and the frequency spectrum (b), with $k_\parallel \rho_i = 0.1$ and $k_\perp \rho_i = 0.55$.

Thus the net number of particles crossing the boundaries of the ith segment in the positive x direction in each time step becomes

$$N^i_{\rm net} = \Gamma^i \delta y \Delta t,$$

where δy and Δt are the widths of the segment and the time step respectively. In each time step, we count the numbers of particles going out of the left, $N^{i,\rm left}_{\rm out}$, and right, $N^{i,\rm right}_{\rm out}$, boundaries of the ith segment, and calculate the numbers of particles injected from the left, $N^{i,\rm left}_{\rm in}$, and right, $N^{i,\rm right}_{\rm in}$, boundaries of the ith segment from the equations

$$N^{i,\rm left}_{\rm in} = N^i_{\rm net} - N^{i,\rm left}_{\rm out}, \tag{2.1}$$

$$N^{i,\rm right}_{\rm in} = N^{i,\rm right}_{\rm out} - N^i_{\rm net}. \tag{2.2}$$

Here the velocities of injected particles are generated using the cumulative distribution function (Birdsall and Langdon 1985).

Since the total number of particles in the system is kept constant in time, the total charge in the system is also kept constant, and set equal to zero. Thus the x components of the electric field at the left and right boundaries can be fixed to zero.

3. Electrostatic ion cyclotron instability

The developed $2\frac{1}{2}$-dimensional open boundary particle simulation model is applied to study current-driven electrostatic ion cyclotron instability. The external uniform magnetic field points in the positive x direction. The open-boundary condition is applied for electrons, while the reflection boundary condition is applied for ions. This is because we assume shifted Maxwellian electrons and non-shifted Maxwellian ions.

The ion motion is followed in three-dimensional velocity space and two-dimensional real space to track the ion cyclotron motion, whereas we adopt the

https://doi.org/10.1017/S0022377899007539 Published online by Cambridge University Press

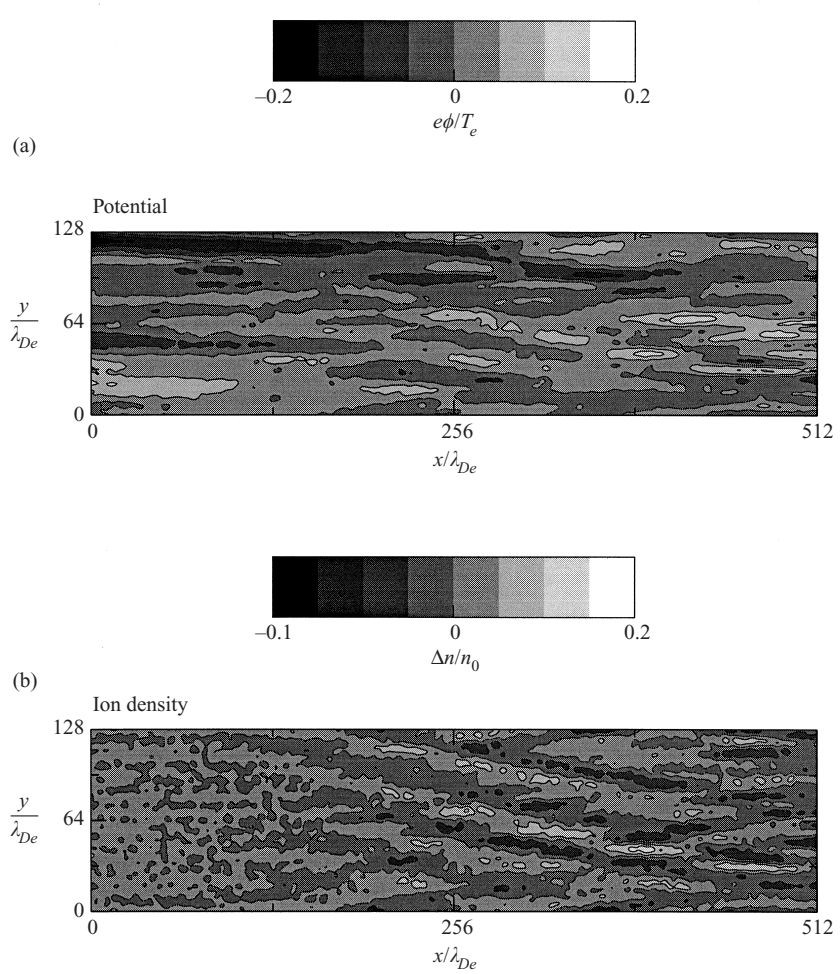


Figure 3. Grey-scale contour plot of the potential (a) and ion density (b) profiles at $\omega_{pe}t = 3000$.

drift kinetic approximation for electrons and trace the electron motion only along the magnetic field lines. This is because the electric field has only x and y components, so $\mathbf{E} \times \mathbf{B}$ drift motion points in the z direction, which is not considered in our model.

We show the simulation results with the following simulation parameters: the system sizes are $L_x = 512\lambda_{De}$ and $L_y = 128\lambda_{De}$ and the grid number is 512×128, where λ_{De} is the Debye length. The system is assumed to be divided into 16 segments in the y direction, and thus the width of each segment is $8\lambda_{De}$. The numbers of ions and electrons are 67 108 864 respectively, and thus 1024 particles per unit grid cell are used. The ion-to-electron mass ratio is 400 and the temperature ratio is $\frac{1}{2}$. The electron cyclotron frequency $\omega_{ce} = 5\omega_{pe}$ and the ion cyclotron frequency $\omega_{ci} = 0.0125\omega_{pe}$, where ω_{pe} is the electron plasma frequency. The electron velocity distribution is a shifted Maxwellian, with drift in the x direction, and the drift velocity is given by $v_{de} = 0.7v_{te}$. Here $v_{te}(= (T_e/m_e)^{1/2})$ is the electron thermal velocity, and T_e and m_e are the electron temperature and mass. The time-step

https://doi.org/10.1017/S0022377899007539 Published online by Cambridge University Press

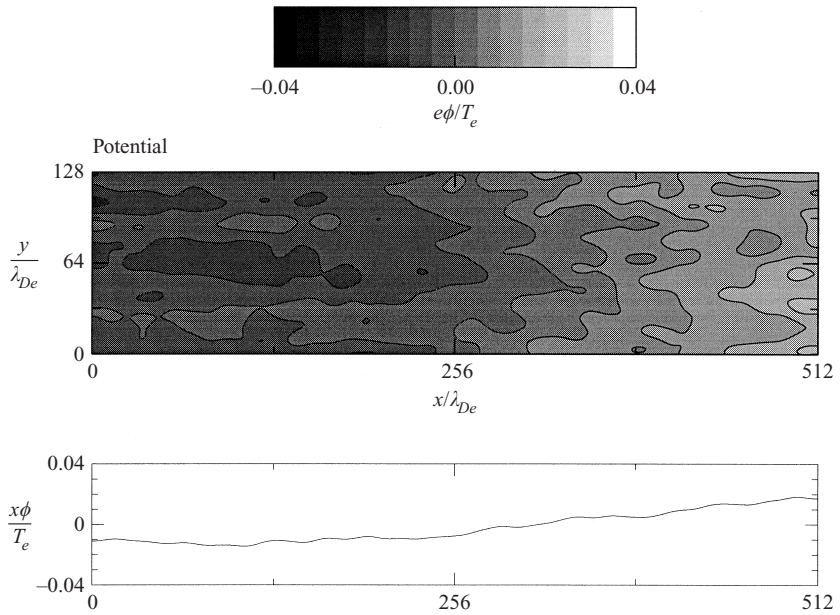


Figure 4. Grey-scale contour plot of the d.c. potential profile at $\omega_{pe}t = 3000$ together with the x-direction profile at $y/\lambda_{De} = 64$.

width $\Delta t = 0.2\omega_{pe}^{-1}$. In a uniform infinite plasma, a linear kinetic dispersion analysis (Kindel and Kennel 1971) predicts that the fundamental modes of the electrostatic ion cyclotron wave with $0.08 \lesssim k_{\|}\rho_i \lesssim 0.18$ and $0.5 \lesssim k_{\perp}\rho_i \lesssim 1.5$ are unstable for the above simulation parameters, while the ion acoustic wave is not unstable.

Figure 2 shows the time evolution of the magnitude of the ion density fluctuation (a) and the frequency spectrum (b) for the mode with $k_{\|}\rho_i = 0.1$ and $k_{\perp}\rho_i = 0.55$, where we use a $\cos k_x x \exp ik_y y$ transform to obtain the spatial spectrum. This is a typical unstable mode for the electrostatic ion cyclotron wave for our choice of simulation parameters as previously described. The peaks of the frequency are around $\omega \approx \pm 1.3\omega_{ci}$, indicating that the mode corresponds to the ion cyclotron wave, which has a phase velocity $\omega/k_{\|} \approx 0.5v_{te}$ and $\omega/k_{\perp} \approx 0.08v_{te}$, and thus propagates at $\pm 80°$ with respect to the magnetic field, with speed $\omega/|k| \approx 0.08v_{te}$.

Figure 3 shows grey-scale contour plots of the potential profile (a) and the ion density profile (b) at $\omega_{pe}t = 3000$, averaged over three times of the plasma period. It is important to note that no sheathlike or any artificial noise appears near the upstream and downstream boundaries, although fresh electrons are supplied from both boundaries. A smeared, intersected wavefront pattern is discernible in the ion density profile for $x/\lambda_{De} \gtrsim 200$. This pattern corresponds to the electrostatic ion cyclotron waves, which propagate almost perpendicularly to the magnetic field lines with a small component of the propagation vector in the positive x direction. The ion cyclotron wave is excited in the upstream region and develops as it propagates from the upstream region to the downstream region. Hence the amplitude in the downstream region is larger than that in the upstream region.

The formation of a d.c. potential due to the instability is shown in Fig. 4. This shows a grey-scale contour plot of the potential profile together with the potential profile along the magnetic field lines at $y = \frac{1}{2}L_y$, which are averaged over the period

https://doi.org/10.1017/S0022377899007539 Published online by Cambridge University Press

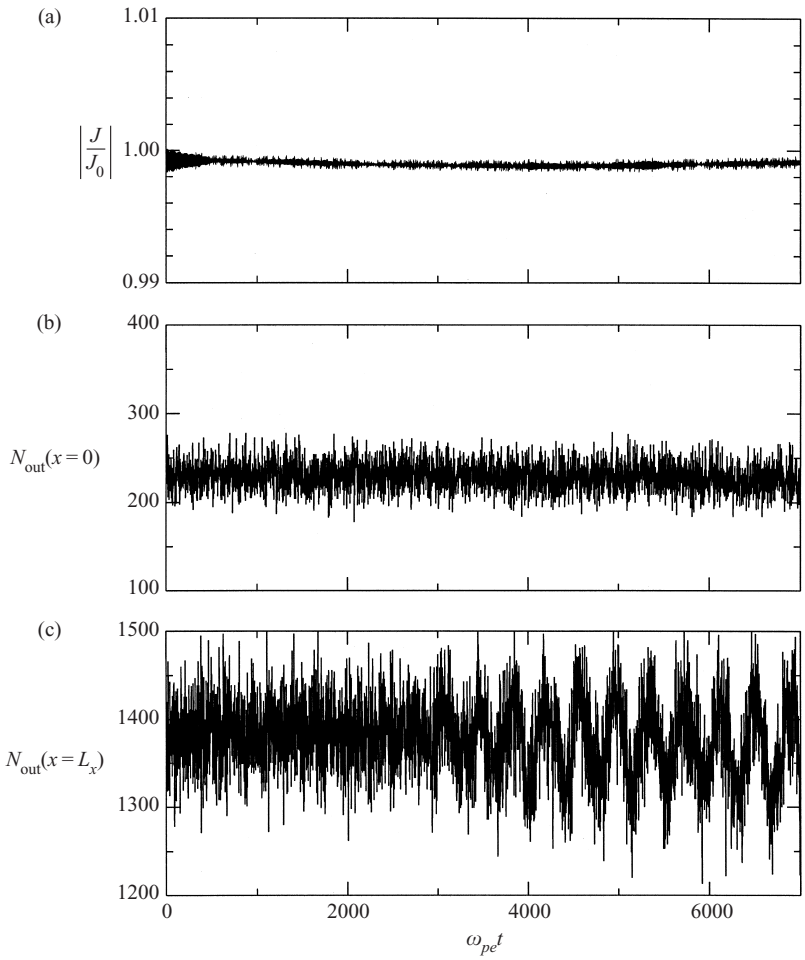


Figure 5. Time history of electron current in the system (a), and the numbers, of outgoing electrons through the left (b) and right (c) boundaries of the fourth segment.

of oscillation of the electrostatic ion cyclotron wave. The potential gradually rises from $x/\lambda_{De} \approx 150$ to the downstream boundary along the magnetic field lines. The potential difference reaches about $e\Delta\phi/T_e \approx 0.03$. This d.c. potential difference is created by the anomalous resistivity due to the instability. The anomalous resistivity can be calculated from the relation $\eta = eE/n_0e^2v_{de} = e(\Delta\phi/L_x)/n_0e^2v_{de}$, resulting in $\eta/\eta_0 \approx 10^{-4}$, where $\eta_0 = 4\pi/\omega_{pe}$.

Figure 5 shows the time evolutions of the electric current (a), and the numbers of outgoing electrons through the left (b) and right (c) boundaries of the fourth segment ($24 < y/\lambda_{De} < 32$). As the ion cyclotron wave grows, the oscillation amplitude of the number of outgoing electrons through the right (downstream) boundary increases. The fundamental frequency of the oscillation is that of the ion cyclotron wave. In spite of this large amplitude oscillation, the electric current through the system remains constant in time.

https://doi.org/10.1017/S0022377899007539 Published online by Cambridge University Press

4. Summary and discussion

We have developed a $2\frac{1}{2}$-dimensional electrostatic open boundary particle simulation code and have shown that the current-driven electrostatic ion cyclotron instability is properly simulated. This open boundary model can smoothly inject fresh particles from the boundary without creating unphysical noise. Furthermore, this simulation succeeded in presenting not only a wavefront pattern accompanied by the ion cyclotron wave, which has been shown in our previous periodic boundary simulation (Ishiguro et al. 1997a), but also the creation of a d.c. potential difference along the magnetic field lines. In this paper we have shown the results for the case with a spatially uniform electron stream. We have also investigated a case with a bell-shaped electron stream, and have succeeded in demonstrating that a V-shaped d.c. potential structure is created by the current-driven electrostatic ion-cyclotron instability(Ishiguro et al. 1997b).

In the usual Q-machine experiments, a positive potential is applied to a small electrode in the plasma to induce an electric current, so the electric field has not only a component along the magnetic field lines, but also a component across these lines. This has given rise to many arguments about the generation mechanism of the oscillation in Q-machine experiments (Hatakeyama et al. 1985; Sato and Hatakeyama 1985; Ishiguro et al. 1994). However, the propagation property reported by Cartier et al. (1985) is consistent with the wavefront pattern observed in the case with a bell-shaped electron stream (Ishiguro et al. 1997a,b).

In our $2\frac{1}{2}$-dimensional configuration, ion $\mathbf{E} \times \mathbf{B}$ drift motion points in the z direction, which is not considered; thus the ion transport due to this drift is not included. It is interesting to investigate how this drift affects the d.c. potential structure by performing a full three-dimensional simulation. This is an issue for future work.

Acknowledgements

The authors would like to thank to Professor C. K. Birdsall for his interest. One of the authors (S. I.) would also like to thank to Professor N. Sato and Professor R. Hatakeyama for their encouragement. The computations were performed by the Advanced Computation System for Complexity at the National Institute for Fusion Science and the Super Computer System at the Computer Centre at Tohoku University.

References

Barnes, C, Hudson, M. K. and Lotko, W. 1985 Weak double layers in ion-acoustic turbulence. *Phys. Fluids* **28**, 1055–1062.

Birdsall, C. K. and Langdon, A. B. 1985 *Plasma Physics via Computer Simulation*. McGraw-Hill, New York.

Cartier, S. L., D'Angelo, N. and Merlino, R. L. 1985 Electrostatic ion-cyclotron waves in a nonuniform magnetic field. *Phys. Fluids* **28**, 3066–3073.

Correll, D. L., Rynn, N. and Böhmer, H. 1975 Onset, growth and saturation of the current-driven ion cyclotron instability. *Phys. Fluids* **18**, 1800–1808.

D'Angelo, N. and Motley, R. W. 1962 Electrostatic oscillations near the ion cyclotron frequency. *Phys. Fluids* **5**, 633–634.

Drummond, W. E. and Rosenbluth, M. N. 1962 Anomalous diffusion arising from microinstabilities in a plasma. *Phys. Fluids* **5**, 1507–1513.

https://doi.org/10.1017/S0022377899007539 Published online by Cambridge University Press

Hatakeyama, R., Muto, F. and Sato, N. 1985 Measurements of potential-driven electrostatic ion cyclotron oscillations in a plasma. *Jpn J. Appl. Phys.* **24**, L285–L287.

Ishiguro, S., Suzawa, Y. and Sato, N. 1994 Potential-driven ion cyclotron oscillations in a magnetized collisionless plasma. *J. Phys. Soc. Jpn* **63**, 3651–3656.

Ishiguro, S., Sato, T., Takamaru, H., Watanabe, K. and the Complexity Simulation Group 1997a Formation of wave-front pattern accompanied by current-driven electrostatic ion-cyclotron instabilities. *Phys. Plasmas* **4**, 2886–2892.

Ishiguro, S., Sato, T., Takamaru, H. and the Complexity Simulation Group 1997b V-Shaped dc potential structure caused by current-driven electrostatic ion-cyclotron instability. *Phys. Rev. Lett.* **78**, 4761–4764.

Kindel, J. M. and Kennel, C. F. 1971 Topside current instabilities. *J. Geophys. Res.* **76**, 3055–3078.

Kintner, P. M., Kelley, M. C. and Mozer, F. S. 1978 Electrostatic hydrogen cyclotron waves near one earth radius altitude in the polar magnetosphere. *Geohys. Res. Lett.* **5**, 139–142.

Kintner, P. M., Kelley, M. C., Sharp, R. D., Ghielmetti, A. G., Temerin, M., Cattell, C., Mizera, P. F. and Fennell, J. F. 1979 Simultaneous observations of energetic (KeV) upstreaming and electrostatic hydrogen cyclotron waves. *J. Geophys. Res.* **84**, 7201–7212.

McWilliams, R., Okubo, M. K. and Wolf, N. S. 1986 Electrostatic ion cyclotron instability near threshold. *Phys. Plasmas* **29**, 3031–3035.

Motley, R. W. and D'Angelo, N 1963 Excitation of electrostatic plasma oscillations near the ion cyclotron frequency. *Phys. Fluids* **6**, 296–299.

Mozer, F. S., Carlson, C. W., Hudson, M. K., Torbert, R. B., Parady, B., Yatteau, J. and Kelley, M. C. 1977 Observations of paired electrostatic shocks in the polar magnetosphere. *Phys. Rev. Lett.* **38**, 292–295.

Okuda, H. Cheng, C. Z. and Lee, W. W. 1981 Numerical simulations of electrostatic hydrogen cyclotron instabilities. *Phys. Fluids* **24**, 1060–1068.

Pritchett, P. L., Ashour-Abdalla, M. and Dawson, J. M. 1981 Simulation of the current-driven electrostatic ion cyclotron instability. *Geophys. Res. Lett.* **8**, 611–613.

Rynn, N., Dakin, D. R., Correll, D. L. and Benford, G. 1974 Ion heating by the current-driven electrostatic ion-cyclotron instability. *Phys. Rev. Lett.* **33**, 765–768.

Sato, T., Takamaru, H., Watanabe, K., Horiuchi, R. and the Complexity Simulation Group 1995 Kinetic self-organization: Creation of super ion-acoustic double layer. *Phys. Plasmas* **2**, 3609–3613.

Sato, N. and Hatakeyama, R. 1985 A mechanism for potential-driven electrostatic ion cyclotron oscillations in a plasma. *J. Phys. Soc. Jpn* **54**, 1661–1664.

Takamaru, H., Sato, T., Horiuchi, R., Watanabe, K. and the Complexity Simulation Group 1997 A self-consistent open boundary model for particle simulation in plasmas. *J. Phys. Soc. Jpn* **66**, 3826–3830.

https://doi.org/10.1017/S0022377899007539 Published online by Cambridge University Press